Therapeutic Discovery

Molecular Cancer Therapeutics

Impact of Intrinsic Affinity on Functional Binding and Biological Activity of EGFR Antibodies

Yu Zhou[1], Anne-Laure Goenaga[1], Brian D. Harms[2], Hao Zou[1], Jianlong Lou[1], Fraser Conrad[1], Gregory P. Adams[3], Birgit Schoeberl[2], Ulrik B. Nielsen[2], and James D. Marks[1]

Abstract

Aberrant expression and activation of EGF receptor (EGFR) has been implicated in the development and progression of many human cancers. As such, targeted therapeutic inhibition of EGFR, for example by antibodies, is a promising anticancer strategy. The overall efficacy of antibody therapies results from the complex interplay between affinity, valence, tumor penetration and retention, and signaling inhibition. To gain better insight into this relationship, we studied a panel of EGFR single-chain Fv (scFv) antibodies that recognize an identical epitope on EGFR but bind with intrinsic monovalent affinities varying by 280-fold. The scFv were converted to Fab and IgG formats, and investigated for their ability to bind EGFR, compete with EGF binding, and inhibit EGF-mediated downstream signaling and proliferation. We observed that the apparent EGFR-binding affinity for bivalent IgG plateaus at intermediate values of intrinsic affinity of the cognate Fab, leading to a biphasic curve describing the ratio of IgG to Fab affinity. Mathematical modeling of antibody–receptor binding indicated that the biphasic effect results from nonequilibrium assay limitations. This was confirmed by further observation that the potency of EGF competition for antibody binding to EGFR improved with both intrinsic affinity and antibody valence. Similarly, both higher intrinsic affinity and bivalent binding improved the potency of antibodies in blocking cellular signaling and proliferation. Overall, our work indicates that higher intrinsic affinity combined with bivalent binding can achieve avidity that leads to greater *in vitro* potency of antibodies, which may translate into greater therapeutic efficacy. *Mol Cancer Ther; 11(7); 1467–76*. *©2012 AACR.*

Introduction

EGF stimulates cell proliferation in normal tissue and in malignant lesions by activating EGF receptor (EGFR) tyrosine kinase signaling pathways (1–3). EGFR is frequently overexpressed in many cancers including breast, colon, head and neck, glioblastoma, gastric, and squamous cell carcinoma (4, 5) and is associated with more aggressive cancer subtypes (6, 7). Anti-EGFR monoclonal antibodies cetuximab and panitumumab are used to treat metastatic colorectal cancers as a single agent or in combination with chemotherapy (8, 9). Both cetuximab and panitumumab inhibit cancer cell proliferation by blocking EGF signaling (10–13) although they can induce immune effector functions as well (14, 15).

Antibodies are attractive candidates for cancer therapeutics not only because of their exquisite specificity to the target and ability to inhibit cell signaling, but also because of their long half-life in serum and the ability to induce tumor antigen-specific immune responses (11, 16). Previously, studies of antibody mechanism of action have revealed insights useful for guiding the engineering of therapeutic antibodies to enhance their antitumor effects, including the importance of target downregulation and signaling blockade by antibody (11, 17), the requirement of Fc to activate Fc receptors for *in vivo* efficacy (18), and the impact of antibody affinity and avidity on *in vivo* tumor targeting (19–22). With respect to antibody affinity effects on tumor targeting, studies have shown that increased binding affinity and valence leads to improved targeting of tumoral vasculature (22). However, we and others have shown that tumor targeting is maximized for antibodies with intrinsic monovalent affinities of K_D in the 1 to 10 nmol/L range, regardless of whether the targeting antibody is a small single-chain Fv (scFv) or bivalent diabody or IgG (19, 21, 23–27). In fact, high affinity IgG that bind internalizing receptors may be more rapidly degraded in tumors than lower affinity IgG, limiting tumor penetration (28). These so called "binding site

Authors' Affiliations: [1]Department of Anesthesia, University of California, San Francisco, San Francisco General Hospital, San Francisco, California; [2]Merrimack Pharmaceuticals, Cambridge, Massachusetts; and [3]Developmental Therapeutics Program, Fox Chase Cancer Center, Philadelphia, Pennsylvania

Note: Supplementary material for this article is available at Molecular Cancer Therapeutics Online (http://mct.aacrjournals.org/).

Corresponding Author: James D. Marks, Department of Anesthesia, University of California, San Francisco, Rm 3C-38, San Francisco General Hospital, 1001 Potrero Avenue, San Francisco, CA 94110. Phone: 415-206-3256; Fax: 415-206-3253; E-mail: marksj@anesthesia.ucsf.edu

doi: 10.1158/1535-7163.MCT-11-1038

barriers" (29–31) may result in higher affinity antibodies having lower quantitative tumor delivery.

Despite the presence of a number of studies examining the impact of affinity and valence on *in vivo* targeting, we can find no data on the impact of intrinsic and apparent affinity on biologic activities of antibodies where the antibody affinity variants bind identical epitopes on the tumor antigen. This knowledge is especially crucial for EGFR-targeting antibodies as their clinical efficacy is thought to rely substantially on the ability to inhibit EGFR-driven cell signaling and proliferation. Therefore, for this work we studied a panel of EGFR scFv antibodies, which varied 280-fold in intrinsic affinity and bound an identical EGFR epitope. By creating Fab and IgG from the scFv, we could dissect the importance of intrinsic affinity and valence-mediated avidity on tumor cell binding, EGFR phosphorylation, and inhibition of tumor cell proliferation.

Materials and Methods

Cell lines

A431, MDAMB468, and MDAMB231 cells were purchased from the American Type Culture Collection (March 2001) and cultured in RPMI 10% FBS and L15 10% FBS media, respectively. Although the cells were not authenticated and tested, mycoplasma contamination was checked regularly.

Antigen and antibodies

Recombinant EGFR-ECD was expressed and purified as previously described (32). Control antibodies include anti-EGFR antibody C225 (cetuximab, Erbitux; Lilly; ref. 11), anti-HER2 antibody C6.5 and anti-BoNT antibody 3D12 (33–35). Anti-EGFR antibody Ab11 (NeoMarkers/LabVision) was used for K_D measurement by KinExA and Ab12 (NeoMarkers/LabVision) for EGFR detection by Western blotting.

Production of anti-EGFR affinity mutant scFv, IgG, and Fab fragments

scFvs with varying affinities for EGFR (36) were subcloned from the yeast-display vector pYD2 (37) via *Nco*I-*Not*I into expression vector pSyn1 for scFv expression or for IgG expression (33). scFvs were produced in the periplasm of *Escherichia coli* strain TG1, and purified by osmotic shock and immobilized metal affinity chromatography, as reported previously (38). Monomeric scFv were separated from dimeric and aggregated scFv by size-exclusion chromatography (Sephadex G75; Amersham Pharmacia) with PBS as eluant. IgG proteins were secreted in the media by transfected CHO cells as described previously (33) and purified by Protein G affinity chromatography (Amersham Pharmacia). Fab fragments were generated by papain digestion (Pierce) of the corresponding IgG followed by separation using Mono S ion-exchange chromatography (GE Healthcare). The homogeneity and purity of the protein preparations were verified by SDS-PAGE stained with Coomassie blue; protein concentrations were measured by microbicinchoninic acid assay (Pierce).

Cell surface–binding measurements

Cell lines that express EGFR were grown to 80% to 90% confluence in their respective media supplemented with 10% FBS and harvested by trypsinization. Each scFv, Fab, or IgG was incubated with 5×10^4 cells for 16 hours at the indicated concentration. Cell binding was carried out at 4°C in PBS containing 1% FBS in adequate volume to maintain constant antibody concentration for equilibrium conditions. After 2 washes with 200 μL of PBS, bound scFv was detected by the addition of 100 μL (1 μg/mL) of biotinylated His probe (Santa Cruz Biotechnology) and streptavidin-phycoerythrin (PE; Biosource/Invitrogen); bound IgG was detected by the addition of 100 μL (1 μg/mL) of PE-labeled anti-human Fc-specific $F(ab')_2$ (Jackson Immnuoresearch); bound Fab was detected by the addition of 100 μL (1 μg/mL) of PE-labeled anti-human Fab-specific $F(ab')_2$ (Jackson Immnuoresearch). After incubating 30 minutes at 4°C, the cells were washed twice and resuspended in PBS containing 4% paraformaldehyde. Fluorescence was measured by flow cytometry using a FACS LSRII (Becton Dickinson), and median fluorescence intensity (MFI) was calculated using CellQuest software (Becton Dickinson). Equilibrium constants were determined as described (39), except that values were fitted to the equation $MFI = MFI_{min} + MFI_{max} \times [Ab]/(K_D + [Ab])$ using KaleidaGraph software.

Effects of EGF on the binding of EGFR antibodies to EGFR-overexpressing cells

The binding assay was conducted as described earlier, except that the antibodies were incubated with EGF at the indicated concentration.

Effects of anti-EGFR affinity mutants on cell proliferation

A431 cells were seeded at 3×10^3 cells per well in 96-well plates (Costar) in RPMI media containing 0.5% FBS and incubated for 5 days with the indicated concentrations of scFv, Fab, or IgG, as described in the figure legends. Cell proliferation was assayed as described using MTT staining (40).

Effects of anti-EGFR affinity mutants on blocking EGF signaling

A431 cells were seeded in 0.5% FBS medium without EGF or anti-EGFR antibodies and cultured in 6-well plates. The culture medium was replenished on day 3. After 5 days, the medium was removed and discarded, and the A431 cells were incubated for 15 minutes at 37°C with 10 nmol/L exogenous EGF and anti-EGFR antibodies at different concentrations as indicated. The cells were then washed twice with cold PBS, lysed with Laemmli sample buffer, boiled and aliquots containing equal amounts of protein were resolved by SDS-PAGE.

The proteins were transferred to nitrocellulose and immunoblotted with antiphosphotyrosine antibody PY20 (Upstate Biotechnology). The total EGFR level in each condition was evaluated with anti-EGFR antibody Ab12—a cocktail of 4 anti-EGFR antibodies to both extracellular and intracellular epitopes.

Determination of affinity constant and binding kinetics by KinExA

Affinity studies of antibody and EGFR reaction mixtures were conducted in PBS (pH 7.4) at room temperature with 1 mg/mL bovine serum albumin (BSA) and 0.02% (w/v) sodium azide added as a preservative. Antibody solution was serially diluted into a constant concentration of EGFR sufficient to produce a reasonable signal. The range of antibody concentration was varied at least 10-fold above and below the value of the apparent K_D and antigen concentrations were set below twice the K_D to ensure a K_D controlled experiment. Sample solutions were allowed to come to equilibrium, then each in the series of 13 dilutions was passed over a flow cell containing a 4-mm column of freshly packed NHS-activated Sepharose 4 Fast Flow beads (GE Healthcare) covalently coated with an antibody binding EGFR at the experimental epitope to capture the unbound antigen from solution. An Alexa-647–labeled antibody Ab11 binding EGFR at a separate epitope was then passed over the bead column to detect the proportion of free antigen. Each dilution was tested in duplicate. The equilibrium titration data were fit to a 1:1 reversible binding model using KinExA Pro Software (version 3.0.6; Sapidyne Instruments) to determine the K_D. Antibody–antigen-binding kinetics were also conducted using the KinExA 3000 to quantify the decrease in free antigen as mixtures of antibody and antigen came to equilibrium. A single mixture of antibody solution and EGFR solution was prepared for each interaction and measured on the instrument by being passed in 0.5 mL volumes over a fresh antigen-binding bead pack at intervals of approximately 550 seconds. Free antigen was detected with Alexa-647–labeled anti-EGFR antibody as described earlier. The exponential decrease in the concentration of free antigen as a function of time was fit to a standard bimolecular rate equation using the KinExA Pro software to determine the k_{on}. The k_{off} was calculated from the product of $k_{on} \times K_D$.

Quantification of EGFR cell surface density

EGFR cell surface density was quantified with Quantum Simply Cellular anti-human IgG bead standards (QSC beads; Bangs laboratories). The QSC beads, coated with different density of anti-Human Fc-specific antibody were stained with 1 nmol/L of C225 IgG. At the same time 4×10^5 cells were washed once with PBS, 0.5% BSA, and labeled with the same amount of C225 IgG for 30 minutes at room temperature. The cells and beads were washed twice with PBS, 0.5% BSA, and analyzed by flow cytometry and the EGFR cell surface density was determined by comparing the MFI of cells to the MFI of the beads.

Computational model of IgG binding

For analysis of IgG-binding data, we used a kinetic model that mathematically describes the binding of antibody to cell surface receptor (41). Model simulation generates a dose–response curve describing the amount of cell surface EGFR bound by antibody. The model consists of 2 equations:

$$IgG + EGFR \leftrightarrow IgG:EGFR$$
$$IgG:EGFR + EGFR \leftrightarrow EGFR:IgG:EGFR$$

The first equation describes the monovalent binding of free antibody in the medium to EGFR, whereas the second equation describes avid, bivalent binding of antibody to EGFR. Antibody-induced internalization of EGFR is neglected in the model as cell-binding experiments were carried out at 4°C. Model simulations incorporate experimentally determined parameters describing monovalent antibody-binding kinetics, cell surface receptor expression level, antibody concentration, and incubation time of antibody with cells. Experimentally measured monovalent antibody-binding kinetics (Supplementary Table S1) were used to derive kinetic-binding rates for model simulations as follows. Because the binding kinetics of the lower affinity antibody variants could not be measured accurately via kinetic exclusion assay (KinExA), all antibody variants were assumed to have the same forward rate constant for binding to EGFR as measured for 2224 IgG. The reverse rate constant for each antibody was calculated as the product of the 2224 IgG rate and the ratio of measured cell-binding affinity of the relevant Fab and 2224 Fab (Supplementary Table S2).

Bivalent binding of EGFR on the cell surface is in addition described in the model by a parameter characterizing the ability of the antibody to cross-link receptors. This parameter was determined computationally, based on a least-squares optimization of the model against the experimental binding dose–response curves. All antibodies were assumed to share a common value for this cross-linking parameter. Antibody affinities were calculated for each simulation as described for the experimental cell surface–binding measurements. All computational methods were developed using MATLAB version 7.12 (The Mathworks, Inc.).

Results

EGFR antibodies studied

The human EGFR C10 scFv was previously isolated by selecting a nonimmune human scFv phage antibody library on CHO cells transfected with EGFR (42). C10 bound EGFR expressing A431 cells with a K_D of 264 nmol/L. The affinity of the C10 scFv for EGFR was increased by using yeast display (36). Seven mutant EGFR scFv antibodies (P3/5, P2/1, P2/4, P2/2, 3524, 2124, and 2224) were isolated with affinities ranging from 88.24 to 0.94 nmol/L as measured on A431 cells (Table 1). V_H and V_L genes from scFv were subcloned for expression as human IgG1/lambda isotype IgG, stable CHO cell lines established, and the resulting IgG purified. Fab fragments

Table 1. Comparison of affinities of scFv, Fab, and IgG for binding to EGFR-overexpressing A431 cells

Antibody	scFv K_D, nmol/L	Fab K_D, nmol/L	IgG K_D, nmol/L	K_D (Fab)/K_D (IgG)
C10	263.67	124.23	1.17	106
P3/5	88.24	58.24	0.5	116
P2/1	14.81	25.4	0.012	2,117
P2/4	15.39	25.2	0.0064	3,938
P2/2	17.01	18.1	0.0077	2,351
3524	7.47	15.4	0.012	1,903
2124	9.90	1.31	0.007	187
2224	0.94	1.2	0.007	171
C225	NA	0.013	0.006	2

NOTE: K_D values for binding to cells were determined by fitting the data from Fig. 1 to the Lineweaver–Burk equation.
Abbreviation: NA, not applicable.

were then enzymatically prepared from the IgG molecules. The parental C10 and higher affinity mutant scFv, Fab, and IgG molecules were used in the present studies to evaluate the impact of intrinsic and apparent antigen-binding affinity on *in vitro* biological effects.

Intrinsic and apparent affinities for EGFR antibody binding to EGFR-overexpressing cancer cells

Using flow cytometry, we characterized the binding affinity of scFv-derived EGFR Fab and IgG molecules for cell surface EGFR on A431 cells (Table 1). In all cases, we found that bivalent IgG had higher observed binding affinity than the cognate monovalent Fab. Previous work in our laboratory had indicated that the affinity gain upon conversion from the monovalent to the bivalent format is higher for low affinity binders (21). Here, however, we found that the ratio of IgG to Fab affinities varied in a biphasic fashion (Table 1 and Supplementary Fig. S1). The intermediate affinity Fab P2/4 showed a very large affinity gain (4,000-fold) upon conversion to bivalent IgG, whereas the Fab clones of low (C10) and high (2224) monovalent affinity showed only 100- to 200-fold affinity gains. C225, the highest affinity Fab, showed the lowest improvement as an IgG (only about 2-fold). In comparing the IgG affinities of P2/4, 2224, and C225, we found that IgG of nearly identical apparent affinity can derive from Fab with widely varying intrinsic affinities (over 3 orders of magnitude between C225 and P2/4). The ratio K_D (Fab)/K_D (IgG) represents the improvement of apparent affinity from the bivalent binding. The bivalent binding actually increases the functional concentration of antibody compared with the monovalent form, but this effect will diminish when the k_{off} is slow enough for antibodies with high intrinsic affinities.

To understand this biphasic effect, we developed a simple computational model of IgG binding to free cell surface receptors to simulate the observed binding curves. The model incorporates the experimentally measured IgG binding kinetics (Supplementary Table S1) and EGFR expression levels, as well as experimental details such as experimental incubation time and antibody concentration. The computational model of IgG binding accurately described the affinities measured for the anti-EGFR IgG (Table 2, second column). In addition, the model was

Table 2. Comparison of measured apparent IgG affinities for A431 cells versus affinities calculated by using a mathematical model

IgG	Experimental K_D, nmol/L	Model K_D, nmol/L	Model K_D (equilibrium), nmol/L	K_D (Fab)/K_D (IgG)
C10	1.17	1.5	1.5	82.8
P3/5	0.5	0.054	0.054	1,078
P2/1	0.012	0.0071	0.0051	4,980
P2/4	0.0064	0.0071	0.0051	4,941
P2/2	0.0077	0.0059	0.0034	5,323
3524	0.012	0.0057	0.0026	5,923
2124	0.007	0.0053	0.00033	3,969
2224	0.007	0.0053	0.00031	3,870

NOTE: Fab affinities from Table 1. K_D (Fab)/K_D (IgG) was corrected for nonequilibrium conditions.

used to simulate binding experiments of sufficient time (10,000-hour incubation period in the *in silico* experiment) to assure equilibrium binding conditions. These simulations revealed that equilibrium constants measured for the high affinity antibodies such as 2224 and 2124 were underestimated by more than 10-fold due to insufficient incubation time at low antibody concentrations (Table 2, third column, and Supplementary Fig. S2). Thus, the mathematical modeling of antibody–receptor binding indicates that the biphasic effect is an artifact of assay limitations (Table 2, fourth column). It was not possible to further increase the incubation time of antibody with cells as the requirement for antibody to be in excess over total receptor numbers led to unacceptable cell loss due to a small number of cells in a large incubation volume.

Impact of EGFR density on antibody apparent affinity

To further validate the computational model of antibody binding, we measured the affinity of C10 and 2224 IgG on tumor cells expressing different levels of EGFR (Fig. 1A). We expected that both antibodies would show improvements in observed affinity on cells expressing higher levels of EGFR. EGFR density was determined for A431, MDA-MB-468, and MDA-MB-231 cells using QSC beads (Fig. 1B). For low affinity IgG C10, observed binding strength increased with the receptor density, from $K_D =$ 13.8 nmol/L on MDAMB231 cells to $K_D = 2.2$ nmol/L on A431 cells, showing a correlation between apparent affinity and receptor density. However, for high affinity IgG 2224, we observed that binding strength improved with decreasing EGFR expression: a 5-fold higher apparent affinity was obtained for MDAMB231 cells, which have 10-fold less EGFR than A431 cells.

We found that the computational model of IgG binding was able to recreate the observed dependence of C10 and 2224 IgG binding affinity on EGFR expression level (Supplementary Table S3). Furthermore, the observed equilibrium constants for high affinity antibody 2224 were again underestimated due to insufficient incubation time in the experimental conditions (Supplementary Table S3). The equilibrium constants calculated from the mathematical model are similar for IgG 2224 on all 3 tumor cells despite the 10-fold difference in their receptor density, suggesting a broader targeting spectrum for EGFR-expressing tumors by using higher affinity antibodies.

Impact of EGF on the binding of EGFR antibodies to EGFR-overexpressing cells

Like EGFR antibodies cetuximab and panitumumab (12, 13), the C10 family of antibodies bind an epitope that

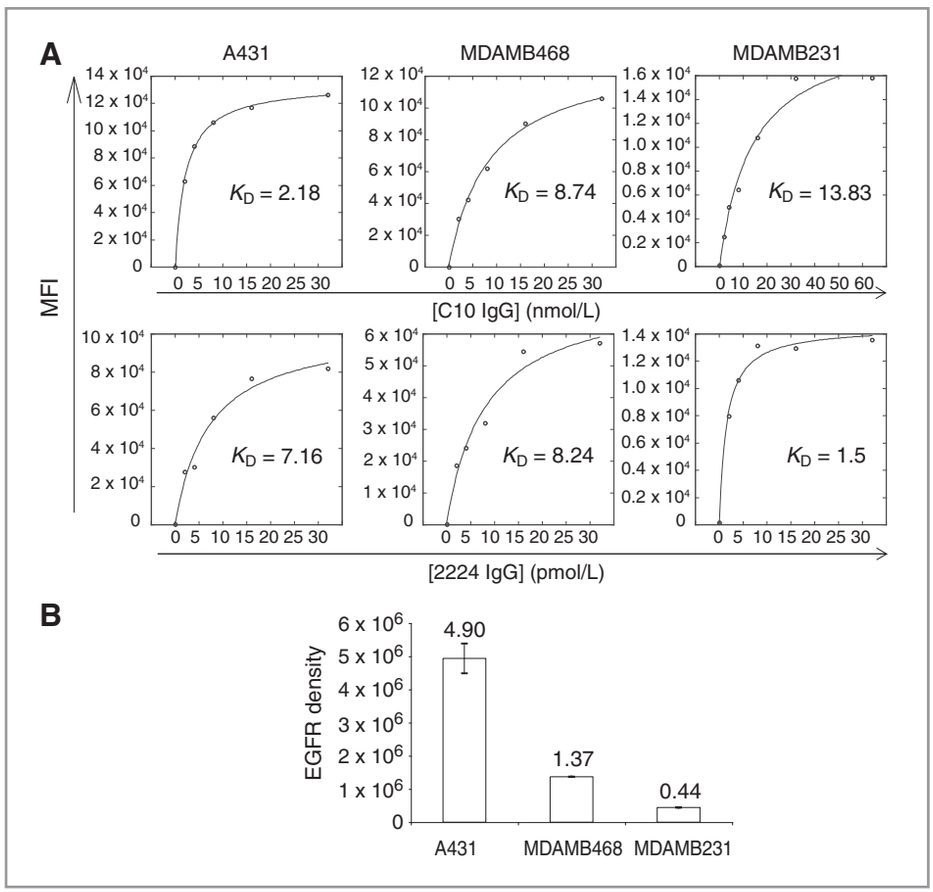

Figure 1. Impact of EGFR density on the apparent binding affinities of IgG to EGFR-overexpressing cells. A, low and high intrinsic affinity IgG (C10 and 2224) had their functional affinities measured on cells of varying EGFR density (B).

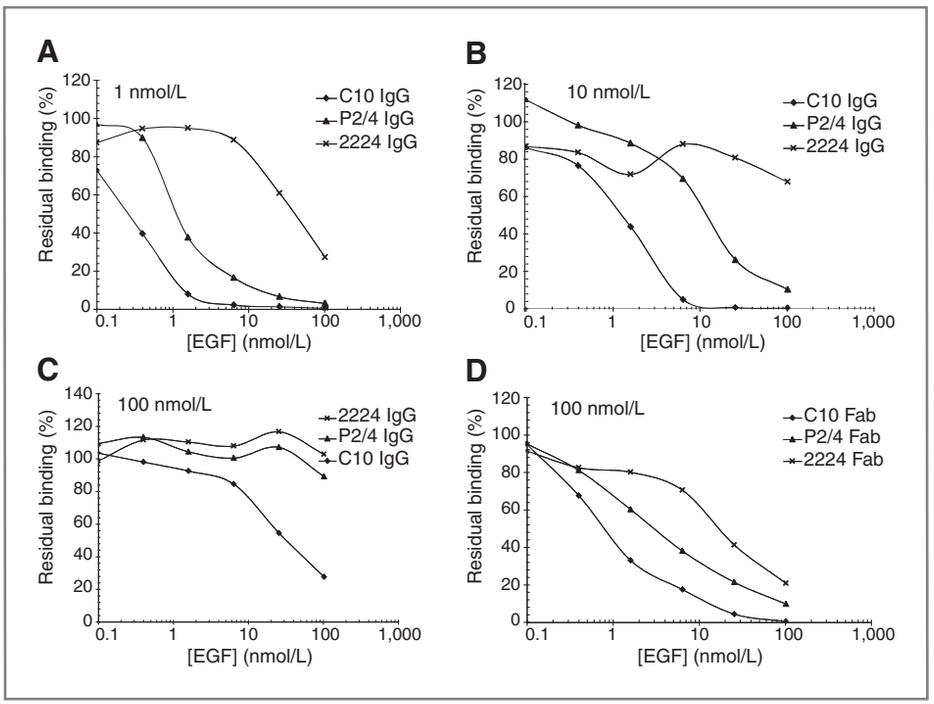

Figure 2. Impact of intrinsic and apparent antibody affinity and concentration on the ability of EGF to inhibit antibody binding to EGFR-overexpressing cells. A, at 1 nmol/L IgG, EGF inhibited the binding of IgG in proportion to their intrinsic affinities; At 10 nmol/L (B) and 100 nmol/L (C) IgG concentration, there was less effect of EGF on IgG binding, especially of the higher intrinsic affinity 2224 and to a lesser extent P2/4. D, EGF inhibited the binding of Fab in proportion to their intrinsic affinities. Comparing C to D, it is clear that an increase in apparent affinity due to IgG avidity significantly reduces the reduction of antibody binding by EGF.

overlaps with the EGF-binding site. As a result, EGF in the local tumor microenvironment could inhibit antibody binding to EGFR and impact tumor targeting. We therefore determined the ability of EGF to compete with IgG antibody binding to EGFR. Using 3 mAbs in the C10 family, we tested IgG at 3 different antibody concentrations (1, 10, and 100 nmol/L) and Fab at 100 nmol/L measuring their binding to A431 cells in the presence of 0.1 to 100 nmol/L of EGF. EGF competitively inhibited the binding of the antibodies to cells (Fig. 2A–D), confirming that the C10 panel of antibodies share an epitope with EGF. For Fab (Fig. 2D), EGF inhibition of Fab binding was proportional to the Fab intrinsic affinity. Bivalent binding of IgG leading to an increased apparent affinity resulted in at least a 10-fold increase in the EGF IC_{50} value for inhibition of antibody binding to cells (Fig. 2C vs. D). However, higher IgG intrinsic affinity also resulted in an increase in the EGF IC_{50} value for inhibition of antibody binding to cells (Fig. 2A vs. B vs. C). For example, P2/4 and 2224 IgG (with similar apparent affinities but 10-fold different intrinsic affinities) differed in their EGF IC_{50} values by approximately 50-fold (Fig. 2A). Thus, EGF IC_{50} values could largely be explained by the relationship between the EGF K_D for binding to EGFR (1 nmol/L) and the intrinsic and apparent affinity of the antibodies.

Impact of intrinsic and apparent affinities on EGF induced EGFR phosphorylation

Enhancement of cell proliferation by EGF occurs via phosphorylation of EGFR and downstream signaling. A previous study has shown that the phosphorylation of EGFR was inhibited more effectively by bivalent form of antibodies than by monovalent Fab fragments (11). We analyzed the antiphosphorylation effect of the C10 panel of EGFR antibodies in both monovalent (scFv) and bivalent (IgG) forms to dissect out the contribution of intrinsic versus apparent affinities. Phosphorylation of EGFR was stimulated by 10 nmol/L EGF. At low antibody concentration relative to EGF concentration (20: 10 nmol/L), inhibition of EGFR phosphorylation was seen only for the IgG and in proportion to the intrinsic affinity (Fig. 3B). At higher antibody: EGF concentration ratios (400:10), inhibition was seen for both scFv and IgG, again in proportion to the intrinsic affinity (Fig. 3A). By comparing the relative inhibition of scFv to the cognate IgG, it is also clear that the increased apparent affinity of the IgG leads to greater inhibition of phosphorylation than the scFv with the same binding site (Fig. 3A, P2/4 and 2224 IgG vs. scFv). As a control, neither the scFv nor IgG of anti-HER2 antibody C6.5 inhibited EGFR phosphorylation, showing target-specific blockade of EGFR activation by anti-EGFR antibodies. No reduction in total EGFR level was observed with the blockade of EGFR activation under the tested condition.

Impact of intrinsic and apparent affinities on antibody antiproliferative capacity

Antibodies against EGFR inhibit the proliferation of cells that overexpress EGFR by blocking the binding of ligands to EGFR (10). To determine the impact of intrinsic and apparent affinity on EGFR antibody anti-proliferative activity, we evaluated the ability of 3 scFv and their cognate IgG to inhibit the growth of A431 cells *in vitro*. The lowest affinity scFv (C10) showed no significant

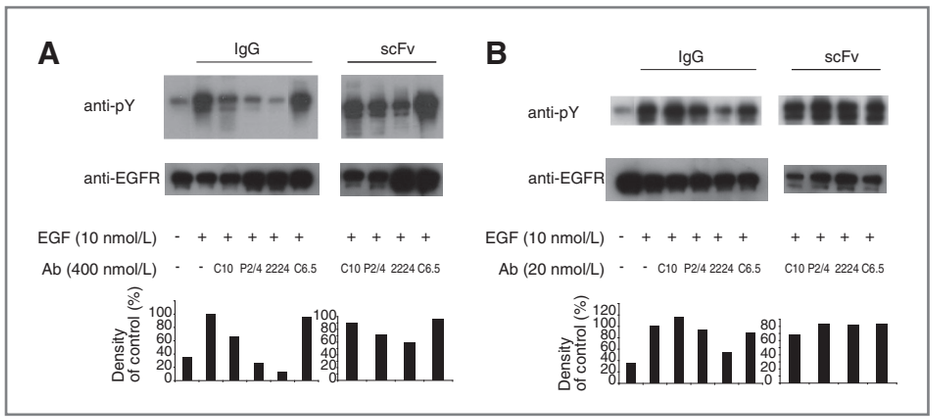

Figure 3. Impact of intrinsic and apparent affinity on EGF induced EGFR phosphorylation. A, increasing scFv intrinsic affinity reduced EGF-induced EGFR phosphorylation; this effect was greatly increased by increasing functional affinity using an IgG constructed from the scFv V-genes. B, at lower antibody concentrations, no effect of scFv on EGF-induced EGFR phosphorylation was observed and the inhibitory effect of the IgG was significantly reduced. Anti-ErbB2 IgG C6.5 was used as the control antibody.

inhibition of A431 proliferation whereas the P2/4 and 2224 scFv inhibited proliferation with IC_{50} values of 300 and 35 nmol/L, respectively (Fig. 4A). Thus, the inhibition of A431 cell growth by the scFv showed a strong correlation with their intrinsic affinities. Likewise, inhibition of proliferation by Fab was greatest for the highest affinity Fab. Fab potency was less than scFv potency (Fig. 4A and B), possibly due to our observation that scFv versions of these antibodies tend to form multivalent aggregates. For the IgG, growth inhibition also correlated with the intrinsic affinity, with a 2.2 nmol/L IC_{50} value for the highest affinity IgG 2224 and more than 160 nmol/L IC_{50} value for the lowest affinity IgG C10 (Fig. 4C). Thus, while P2/4 and 2224 IgG experimentally have comparable apparent affinities, their IC_{50} values for inhibition of proliferation differ by more than 30-fold. The IC_{50} value of the 2224 IgG was also 67-fold less than that of the 2224 Fab and 16-fold lower than the 2224 scFv, which indicated a significant impact of apparent affinity (bivalent binding) on the antiproliferative effect. It is also notable that the impact of the bivalent binding was greater for the IgG with higher intrinsic affinity than the IgG with lower intrinsic affinity. The anti-EGFR antibody C225, which bound the extracellular domain of EGFR with 0.21 nmol/L affinity measured by KinExA (Supplementary Table S1), inhibited the cell proliferation to a similar extent as 2224 for IgG (Fig. 4C) and slightly better than 2224 for Fab form (Fig. 4B). As a negative control, the anti-BoNT antibody 3D12 did not show proliferative inhibition.

Discussion

One of the attractive features of antibodies as therapeutics is the ability to use the tools of antibody engineering to tune affinity, valency, and pharmocokinetics. This allows testing and identification of the optimal antibody properties for a given application. Many therapeutic antibodies in oncology function by binding to cell surface receptors at an epitope, which blocks ligand binding, thus inhibiting receptor activation. While it may seem intuitive that higher antibody affinity for antigen would be beneficial in this setting, no studies have rigorously explored the relationship between affinity, valency, and the ability of antibodies to inhibit signaling and proliferation driven by oncogenic targets like EGFR.

To address this question, we studied EGFR antibodies binding an identical epitope with intrinsic affinities differing by more than 250-fold in monovalent form. Upon conversion of these antibodies to IgG format, we surprisingly observed a biphasic relationship between intrinsic monovalent affinity and bivalent-binding strength. This is in contrast to our previous results using a set of IgG affinity variants targeting HER2 at the same epitope, where we observed a monotonic decline in the observed ratio of intrinsic monovalent K_D to functional bivalent K_D (35). In the current work, we used a computational binding model to successfully predict the observed IgG affinities, and to further show that the biphasic effect results from nonequilibrium experimental conditions that underestimate the actual functional binding strength for the higher affinity antibodies. Similar nonequilibrium effects are also likely present in the results of Tang and colleagues (35) and specific experimental conditions the cause of the different observed relationships between intrinsic and functional affinity. While it might appear that the solution to this measurement problem is to increase incubation time beyond the 16 hours used, such studies are intractable due to poor cell recovery in the large incubation volumes and small numbers of cells needed to ensure antibody excess over receptor number. Fortunately, mathematical modeling allows the prediction of true binding affinities even if experimentally infeasible to measure.

In addition to the cell-binding studies, the anti-EGFR antibodies were analyzed in both monovalent and bivalent forms for their abilities to inhibit cell proliferation and EGF signaling. Signaling and proliferation inhibition by both monomeric scFv and Fab correlated with their monovalent-binding constants, whereas the bivalent IgG exhibited much greater inhibition than comparable affinity monovalent antibodies, due to higher functional affinity. IgG derived from higher intrinsic affinity-binding sites (such as 2224) had greater inhibition of EGFR phosphorylation and cell growth than IgG

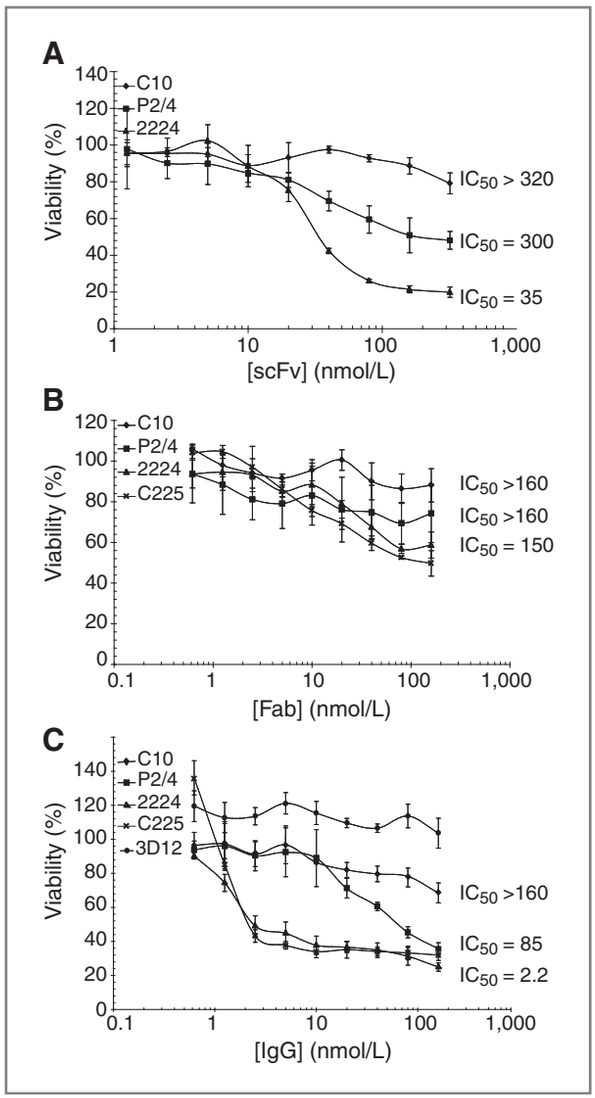

Figure 4. Inhibition of A431 cell proliferation by anti-EGFR scFv, IgG and Fab. A, inhibition of proliferation of A431 cells increased with increasing scFv intrinsic affinity, with an IC_{50} value of 35 nmol/L for the highest affinity 2224 scFv. B, inhibition of proliferation of A431 cells increased with increasing Fab intrinsic affinity, but this effect was less than that observed for the scFv. C, inhibition of proliferation of A431 cells increased with increasing IgG intrinsic affinity. 3D12, control anti-botulinum neurotoxin antibody.

derived from lower intrinsic binding sites (P2/4), even though P2/4 and 2224 had comparable apparent affinities (due to assay limitations). These results indicate that for antibodies that inhibit signaling, both higher intrinsic affinity and avid bivalent binding lead to greater *in vitro* potency.

Whether this results in greater *in vivo* efficacy remains unproven. The overall efficacy of antibody therapies results not only from signaling inhibition, but also from effective tumor penetration and retention and for some targets antibody-dependent cell-mediated cytotoxicity and complement-dependent cytotoxic antibody activity. We and others have shown that for antibodies targeting solid tumors, affinities lower than $K_D = 1$ to 10 nmol/L do not increase quantitative tumor accumulation and may actually reduce the magnitude of tumor targeting (21, 23, 26, 28). In fact, using a series of HER2-targeted antibody variants binding the same epitope with different affinity, we have recently shown that higher affinity antibodies are more rapidly internalized and degraded in tumors than antibodies of lower affinity, limiting tumor penetration (28). This effect was particularly pronounced for the IgG with an intrinsic binding site K_D significantly less than 1 nmol/L. While the EGFR IgG studied did not have intrinsic K_D in this range, such effects are likely to occur for EGFR antibodies, and might be more pronounced due to the faster rate of EGFR internalization relative to HER2. In addition, higher intrinsic affinity could result in greater binding of shed tumor antigen in the tumor microenvironment than in antibodies of lower intrinsic affinity, interfering with cell binding and signaling inhibition. These "binding site barriers" (29–31) for tumor delivery may result in higher affinity antibodies having lower efficacy despite a higher intrinsic ability to inhibit signaling pathways. Experimental *in vivo* evaluation of antibodies binding identical epitopes but with varying intrinsic and functional affinities will help elucidate the impact of these interconnected factors on overall antibody efficacy.

Disclosure of Potential Conflicts of Interest

J.D. Marks has major ownership interest in Merrimack Pharmaceuticals. He also is a consultant and on the scientific advisory board of Merrimack Pharmaceuticals. No potential conflicts of interest were disclosed by the other authors.

Authors' Contributions

Conception and design: Y. Zhou, U.B. Nielsen, J.D. Marks
Development of methodology: Y. Zhou, A.L. Goenaga, B.D. Harms, J. Lou, B. Schoeberl, J.D. Marks
Acquisition of data (provided animals, acquired and managed patients, provided facilities, etc.): A.L. Goenaga, B.D. Harms, H. Zou, J. Lou, F. Conrad
Analysis and interpretation of data (e.g., statistical analysis, biostatistics, computational analysis): Y. Zhou, A.L. Goenaga, B.D. Harms, F. Conrad, J.D. Marks
Writing, review, and/or revision of the manuscript: Y. Zhou, A.L. Goenaga, B.D. Harms, J. Lou, F. Conrad, G.P. Adams, B. Schoeberl, U.B. Nielsen
Administrative, technical, or material support (i.e., reporting or organizing data, constructing databases): H. Zou, F. Conrad
Study supervision: U.B. Nielsen, J.D. Marks
Funding of the antibody generation (part of my NCI grant): G.P. Adams

Grant Support

The study was supported by National Cancer Institute/NIH grant P50 CA58207 (to L.J. Van't Veer) and R01 CA118159 (to G.P. Adams). Financial support was also given to Y. Zhou, A.L. Goenaga, H. Zou, J. Lou, F. Conrad, and J.D. Marks.

The costs of publication of this article were defrayed in part by the payment of page charges. This article must therefore be hereby marked *advertisement* in accordance with 18 U.S.C. Section 1734 solely to indicate this fact.

Received December 20, 2011; revised April 12, 2012; accepted April 30, 2012; published OnlineFirst May 7, 2012.

References

1. Ozanne B, Richards CS, Hendler F, Burns D, Gusterson B. Over-expression of the EGF receptor is a hallmark of squamous cell carcinomas. J Pathol 1986;149:9–14.
2. Di Fiore PP, Pierce JH, Fleming TP, Hazan R, Ullrich A, King CR, et al. Overexpression of the human EGF receptor confers an EGF-dependent transformed phenotype to NIH 3T3 cells. Cell 1987;51:1063–70.
3. Velu TJ, Beguinot L, Vass WC, Willingham MC, Merlino GT, Pastan I, et al. Epidermal-growth-factor-dependent transformation by a human EGF receptor proto-oncogene. Science 1987;238:1408–10.
4. Salomon DS, Brandt R, Ciardiello F, Normanno N. Epidermal growth factor-related peptides and their receptors in human malignancies. Crit Rev Oncol Hematol 1995;19:183–232.
5. Motoyama AB, Hynes NE, Lane HA. The efficacy of ErbB receptor-targeted anticancer therapeutics is influenced by the availability of epidermal growth factor-related peptides. Cancer Res 2002;62:3151–8.
6. Sainsbury JR, Malcolm AJ, Appleton DR, Farndon JR, Harris AL. Presence of epidermal growth factor receptor as an indicator of poor prognosis in patients with breast cancer. J Clin Pathol 1985;38:1225–8.
7. Nielsen TO, Hsu FD, Jensen K, Cheang M, Karaca G, Hu Z, et al. Immunohistochemical and clinical characterization of the basal-like subtype of invasive breast carcinoma. Clin Cancer Res 2004;10:5367–74.
8. Cunningham D, Humblet Y, Siena S, Khayat D, Bleiberg H, Santoro A, et al. Cetuximab monotherapy and cetuximab plus irinotecan in irinotecan-refractory metastatic colorectal cancer. N Engl J Med 2004;351:337–45.
9. Gibson TB, Ranganathan A, Grothey A. Randomized phase III trial results of panitumumab, a fully human anti-epidermal growth factor receptor monoclonal antibody, in metastatic colorectal cancer. Clin Colorectal Cancer 2006;6:29–31.
10. Sato JD, Kawamoto T, Le AD, Mendelsohn J, Polikoff J, Sato GH. Biological effects *in vitro* of monoclonal antibodies to human epidermal growth factor receptors. Mol Biol Med 1983;1:511–29.
11. Fan Z, Masui H, Altas I, Mendelsohn J. Blockade of epidermal growth factor receptor function by bivalent and monovalent fragments of 225 anti-epidermal growth factor receptor monoclonal antibodies. Cancer Res 1993;53:4322–8.
12. Yang XD, Jia XC, Corvalan JR, Wang P, Davis CG, Jakobovits A. Eradication of established tumors by a fully human monoclonal antibody to the epidermal growth factor receptor without concomitant chemotherapy. Cancer Res 1999;59:1236–43.
13. Goldstein NI, Prewett M, Zuklys K, Rockwell P, Mendelsohn J. Biological efficacy of a chimeric antibody to the epidermal growth factor receptor in a human tumor xenograft model. Clin Cancer Res 1995;1:1311–8.
14. Bleeker WK, Lammerts van Bueren JJ, van Ojik HH, Gerritsen AF, Pluyter M, Houtkamp M, et al. Dual mode of action of a human anti-epidermal growth factor receptor monoclonal antibody for cancer therapy. J Immunol 2004;173:4699–707.
15. Schneider-Merck T, Lammerts van Bueren JJ, Berger S, Rossen K, van Berkel PH, Derer S, et al. Human IgG2 antibodies against epidermal growth factor receptor effectively trigger antibody-dependent cellular cytotoxicity but, in contrast to IgG1, only by cells of myeloid lineage. J Immunol 2010;184:512–20.
16. Weiner LM, Dhodapkar MV, Ferrone S. Monoclonal antibodies for cancer immunotherapy. Lancet 2009;373:1033–40.
17. Sliwkowski MX, Lofgren JA, Lewis GD, Hotaling TE, Fendly BM, Fox JA. Nonclinical studies addressing the mechanism of action of trastuzumab (Herceptin). Semin Oncol 1999;26:60–70.
18. Clynes RA, Towers TL, Presta LG, Ravetch JV. Inhibitory Fc receptors modulate *in vivo* cytoxicity against tumor targets. Nat Med 2000;6:443–6.
19. Adams GP, Schier R, Marshall K, Wolf EJ, McCall AM, Marks JD, et al. Increased affinity leads to improved selective tumor delivery of single-chain Fv antibodies. Cancer Res 1998;58:485–90.
20. Adams GP, Schier R, McCall AM, Crawford RS, Wolf EJ, Weiner LM, et al. Prolonged *in vivo* tumour retention of a human diabody targeting the extracellular domain of human HER2/neu. Br J Cancer 1998b;77:1405–12.
21. Nielsen UB, Adams GP, Weiner LM, Marks JD. Targeting of bivalent anti-ErbB2 diabody antibody fragments to tumor cells is independent of the intrinsic antibody affinity. Cancer Res 2000;60:6434–40.
22. Viti F, Tarli L, Giovannoni L, Zardi L, Neri D. Increased binding affinity and valence of recombinant antibody fragments lead to improved targeting of tumoral angiogenesis. Cancer Res 1999;59:347–52.
23. Adams GP, Schier R, McCall AM, Simmons HH, Horak EM, Alpaugh RK, et al. High affinity restricts the localization and tumor penetration of single-chain fv antibody molecules. Cancer Res 2001;61:4750–5.
24. Graff CP, Wittrup KD. Theoretical analysis of antibody targeting of tumor spheroids: importance of dosage for penetration, and affinity for retention. Cancer Res 2003;63:1288–96.
25. Jackson H, Bacon L, Pedley RB, Derbyshire E, Field A, Osbourn J, et al. Antigen specificity and tumour targeting efficiency of a human carcinoembryonic antigen-specific scFv and affinity-matured derivatives. Br J Cancer 1998;78:181–8.
26. Schmidt MM, Thurber GM, Wittrup KD. Kinetics of anti-carcinoembryonic antigen antibody internalization: effects of affinity, bivalency, and stability. Cancer Immunol Immunother 2008;57:1879–90.
27. Thurber GM, Wittrup KD. Quantitative spatiotemporal analysis of antibody fragment diffusion and endocytic consumption in tumor spheroids. Cancer Res 2008;68:3334–41.
28. Rudnick SI, Lou J, Shaller CC, Tang Y, Klein-Szanto AJ, Weiner LM, et al. Influence of affinity and antigen internalization on the uptake and penetration of Anti-HER2 antibodies in solid tumors. Cancer Res 2011;71:2250–9.
29. Fujimori K, Covell DG, Fletcher JE, Weinstein JN. A modeling analysis of monoclonal antibody percolation through tumors: a binding-site barrier. J Nucl Med 1990;31:1191–8.
30. Fujimori K, Covell DG, Fletcher JE, Weinstein JN. Modeling analysis of the global and microscopic distribution of immunoglobulin G, F(ab′)2, and Fab in tumors. Cancer Res 1989;49:5656–63.
31. van Osdol W, Fujimori K, Weinstein JN. An analysis of monoclonal antibody distribution in microscopic tumor nodules: consequences of a "binding site barrier". Cancer Res 1991;51:4776–84.
32. Horak E, Heitner T, Robinson MK, Simmons HH, Garrison J, Russeva M, et al. Isolation of scFvs to *in vitro* produced extracellular domains of EGFR family members. Cancer Biother Radiopharm 2005;20:603–13.
33. Nowakowski A, Wang C, Powers DB, Amersdorfer P, Smith TJ, Montgomery VA, et al. Potent neutralization of botulinum neurotoxin by recombinant oligoclonal antibody. Proc Natl Acad Sci U S A 2002;99:11346–50.
34. Schier R, Marks JD, Wolf EJ, Apell G, Wong C, McCartney JE, et al. *In vitro* and *in vivo* characterization of a human anti-c-erbB-2 single-chain Fv isolated from a filamentous phage antibody library. Immunotechnology 1995;1:73–81.
35. Tang Y, Lou J, Alpaugh RK, Robinson MK, Marks JD, Weiner LM. Regulation of antibody-dependent cellular cytotoxicity by IgG intrinsic and apparent affinity for target antigen. J Immunol 2007;179:2815–23.
36. Zhou Y, Drummond DC, Zou H, Hayes ME, Adams GP, Kirpotin DB, et al. Impact of single-chain Fv antibody fragment affinity on nanoparticle targeting of epidermal growth factor receptor-expressing tumor cells. J Mol Biol 2007;371:934–47.
37. Razai A, Garcia-Rodriguez C, Lou J, Geren IN, Forsyth CM, Robles Y, et al. Molecular evolution of antibody affinity for sensitive detection of botulinum neurotoxin type A. J Mol Biol 2005;351:158–69.
38. Schier R, Bye J, Apell G, McCall A, Adams GP, Malmqvist M, et al. Isolation of high-affinity monomeric human anti-c-erbB-2 single chain Fv using affinity-driven selection. J Mol Biol 1996;255:28–43.

39. Benedict CA, MacKrell AJ, Anderson WF. Determination of the binding affinity of an anti-CD34 single-chain antibody using a novel, flow cytometry based assay. J Immunol Methods 1997; 201:223–31.
40. Alley MC, Scudiero DA, Monks A, Hursey ML, Czerwinski MJ, Fine DL, et al. Feasibility of drug screening with panels of human tumor cell lines using a microculture tetrazolium assay. Cancer Res 1988;48:589–601.
41. Harms BD, Kearns JD, Su SV, Kohli N, Nielsen UB, Schoeberl B. Optimizing properties of antireceptor antibodies using kinetic computational models and experiments. Methods Enzymol 2012; 502:67–87.
42. Heitner T, Moor A, Garrison JL, Marks C, Hasan T, Marks JD. Selection of cell binding and internalizing epidermal growth factor receptor antibodies from a phage display library. J Immunol Methods 2001;248:17–30.